Cross-Dataset Analysis of PPG Feature Correlations with Blood Pressure Targets

Matteo Ricci[1,2], Arturo Martínez-Rodrigo[3], Raúl Alcaraz[3], Frida Sandberg[2], José J. Rieta[1]
[1]Electronic Engineering Department, Universitat Politècnica de València, Valencia, Spain
[2]Department of Biomedical Engineering, Lund University, Lund, Sweden
[3]Res. Group in Electronic, Biomed. and Telecomm. Eng., University of Castilla-La Mancha, Spain

Abstract

Photoplethysmography (PPG) is a low-cost, non-invasive technology studied for blood pressure (BP) estimation, but the cross-cohort consistency of its morphology–BP associations remains uncertain. We evaluated the cross-dataset consistency of 41 PPG-feature correlations with SBP/DBP in PPG-BP, VitalDB, MIMIC-III-Ext-PPG, and MIMIC-IV Waveform. Up to three segments per subject (30 s for VitalDB/MIMIC, 2.1 s for PPG-BP) were retained if physiologically plausible and morphologically consistent. Subject-level Spearman correlations (ρ) with SBP and DBP were computed per dataset and summarized by mean, minimum, and range. Twenty-two features reached mean $|\rho| > 0.3$ for SBP and 15 for DBP. Consistent SBP correlates included signed SDPTG ratios b/a and d/a, PDA-A_{13}, and AI_{gh}; timing and slope features were more cohort-dependent. These findings support feature screening for cross-dataset BP modeling, without establishing predictive performance or causality.

1. Introduction

Photoplethysmography (PPG) is widely investigated for cuffless blood pressure (BP) estimation because it is inexpensive, non-invasive, and sensitive to peripheral hemodynamic variation [1–3]. Many approaches therefore extract timing, amplitude, derivative, and pulse-decomposition descriptors from the PPG waveform and use them to estimate systolic and diastolic BP [4, 5]. Such features are attractive because they are interpretable, computationally lightweight, and can be obtained from a single optical signal without an electrocardiogram or calibration waveform.

A major barrier to generalization is cohort heterogeneity. Public PPG datasets differ in demographics, disease severity, measurement modality, and acquisition environment, ranging from controlled ambulatory recordings to intraoperative and intensive-care monitoring [6, 7]. These differences affect signal quality, vascular tone, medication exposure, and BP measurement type. Consequently, features that correlate with BP in one population may show weaker or different associations in another, limiting model transferability and motivating explicit cross-dataset assessment [8]. This is especially important because high within-dataset correlations can be misleading if they reflect cohort-specific physiology or acquisition protocols rather than consistent cardiovascular information.

This study evaluates the consistency of PPG feature correlations with SBP and DBP across four heterogeneous clinical datasets [9, 10]. Rather than validating a predictive model, the aim is to identify candidate features with consistent cross-dataset association magnitudes, define a reproducible consistency rule, and highlight features whose behavior appears cohort-dependent before they are prioritized in generalizable BP estimation algorithms [11]. The analysis focuses on absolute Spearman correlation to compare association strength across cohorts, while explicitly noting that signed correlations are still required for physiological interpretation.

2. Material and Methods

We analyzed data from four public sources to capture different physiological states and acquisition conditions: PPG-BP [12] (219 ambulatory subjects), VitalDB [13] (285 intraoperative subjects), MIMIC-III-Ext-PPG [14] (225 ICU subjects), and MIMIC-IV Waveform [15] (63 ICU subjects). The term selected is used because no formal demographic or hemodynamic representativeness analysis against the full databases was performed; instead, subject inclusion was purely driven by the signal quality and stationarity criteria described below.

Up to three 30-s segments per subject were extracted from VitalDB, MIMIC-III, and MIMIC-IV under stationary conditions. Segments were selected using three criteria: (i) heart rate between 40 and 180 bpm; (ii) cardiac spectral dominance, defined as a ratio > 0.8 between the power in the 0.5–4 Hz band and the total signal power; and (iii) rhythmic stability with an interbeat-interval coefficient of variation < 0.10 [16]. These stationary segments were then paired with synchronized invasive arterial BP targets.

For the ambulatory cohort, PPG-BP retained its native 2.1-s segments and accompanying non-invasive cuff SBP/DBP values.

Raw PPG signals were bandpass-filtered at 0.5–12 Hz. Forty-one pulse-level morphology features were then extracted. These included landmark timings (t_x) and amplitudes (A_x), normalized time intervals between landmarks ($\Delta n_{xy} = (t_y - t_x)/T$, where T is the pulse period), pulse widths at 30–90%, Inflection Point Area (IPA), signed SDPTG ratios b/a, c/a, d/a, and e/a, the aging index $AX = (b - c - d - e)/a$, wave-reflection descriptors such as $AI_{gh} = (A_g - A_h)/A_g$ and $Y_{gh} = A_h/A_g$, and Pulse Decomposition Analysis (PDA) timing, amplitude, and width descriptors, including PDA-A_{13}, PDA-T_{13}, PDA-T_{14}, PDA-T_{15}, and PDA-W_1 [8, 17].

Segments were discarded when their median feature variability index exceeded 0.3. Following the variability assessment proposed in our concurrent work [18], this index quantifies within-segment morphological consistency. It is calculated for each segment as the median of the intra-segment standard deviations of all extracted features, normalized by their respective global standard deviations within the dataset. The global standard deviations were computed after physiological screening and before applying the rejection rule.

Spearman correlations were computed at the subject level after taking the median of the segment-level medians for each subject, thereby reducing pseudo-replication from repeated segments. Absolute correlations were used to summarize and rank association magnitudes by mean $|\rho|$, minimum $|\rho|$, and min–max range across datasets. A feature was labeled consistent if its minimum $|\rho| > 0.30$ and its range ≤ 0.20; features with high mean magnitude but wider ranges were considered variable. It is important to note that all features identified as consistent maintained the same correlation direction across the four cohorts. In addition, relying on minimum magnitude and range prevents features with one weak cohort from being falsely classified as robust.

3. Results

The variability threshold retained 89.3% of PPG-BP segments, 70.9% of VitalDB, 55.4% of MIMIC-III, and 62.5% of MIMIC-IV (Figure 1), consistent with greater signal complexity in ICU recordings.

Using the mean-magnitude criterion, 22 features reached mean $|\rho| > 0.30$ for SBP and 15 for DBP; the stricter consistent label in Table 1 also required minimum $|\rho| > 0.30$ and range ≤ 0.20. For SBP, the strongest consistent correlates were b/a (mean $|\rho| = 0.71$, range 0.59–0.78), d/a (0.65, 0.59–0.71), PDA-A_{13} (0.65, 0.62–0.75), AX (0.63, 0.60–0.66), and AI_{gh} (0.56, 0.51–0.62). These features remained above the threshold in all cohorts,

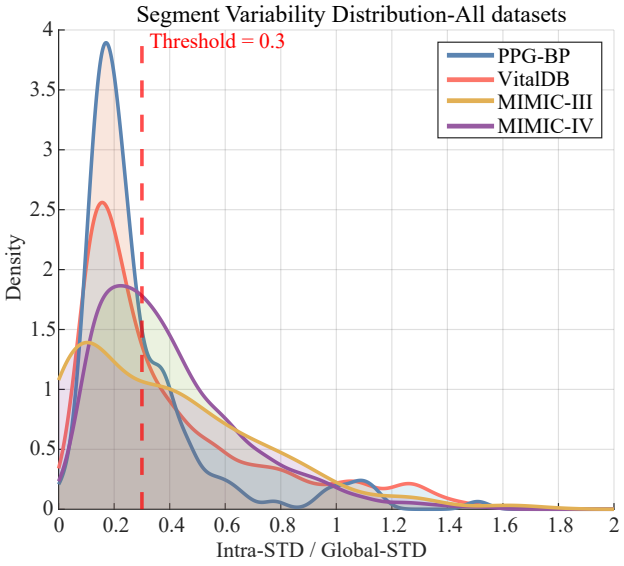

Figure 1: Density distribution of the intra-segment variability ratio across the four datasets. The dashed red line indicates the 0.3 rejection threshold.

suggesting that SDPTG morphology, selected PDA amplitudes, and wave-reflection descriptors preserve association magnitude better than many timing variables. The consistency of b/a, d/a, and AX is also coherent with their common use as descriptors of vascular aging or arterial stiffness, although the present analysis only demonstrates correlation consistency. Figure 2a visualizes the five most consistent non-PDA SBP features by mean $|\rho|$, complementing the PDA-inclusive ranking in Table 1.

DBP showed lower overall correlation magnitudes. The strongest consistent correlates for DBP were Δn_{pf}, PDA-W_1, Δn_{up}, N_e, Δn_{ue}, and Δn_{gh}, with mean $|\rho|$ values between 0.44 and 0.49. This narrower dynamic range indicates that DBP may require additional information beyond isolated morphology features, particularly when moving between ambulatory, surgical, and ICU cohorts. It also cautions against assuming that features selected for SBP will transfer directly to DBP, since DBP is more closely linked to vascular resistance and peripheral runoff than to peak systolic morphology alone.

Variable features (Table 1) had acceptable mean $|\rho|$ but exceeded the consistency range criterion, including S_{pf}, Δn_{pf} (which also fell below the minimum threshold), and the PDA timing descriptors PDA-T_{13}–T_{15}, even when their rounded minimum values remained above 0.30. These patterns suggest sensitivity to acquisition protocol, vascular state, or ICU-specific clinical factors, including vasoactive medication, autonomic tone, diagnosis mix, and the use of invasive rather than cuff BP targets. Overall, the results support using consistent features for model design but should be interpreted as feature-screening evidence rather

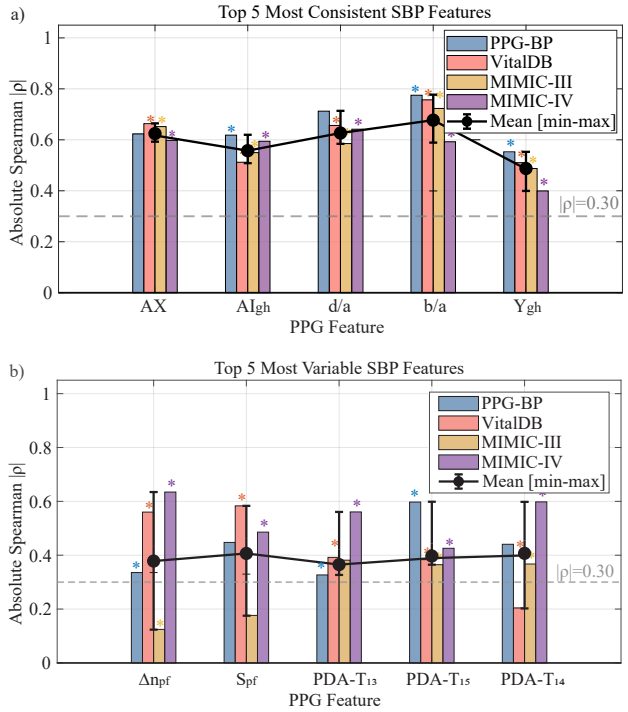

Figure 2: (a) Five consistent non-PDA SBP features shown as a visual summary; the PDA-inclusive ranking is reported in Table 1. (b) Five SBP features with high mean $|\rho|$ but wide cross-dataset ranges. Asterisks indicate uncorrected $p < 0.05$.

than predictive validation. The table also shows why the consistency definition must include both minimum correlation and range: several variables have acceptable mean values, but a single weak cohort would limit direct transfer to unseen populations. The analysis deliberately prioritizes reproducibility of feature behavior over model accuracy; a feature with consistent correlation may still fail in a multivariable model, whereas an unstable feature may remain useful after cohort calibration or domain adaptation.

4. Discussion

While our analysis identifies candidate PPG features for cross-dataset BP modeling, it is important to note that $|\rho|$ summarizes association magnitude only and does not prove direction, predictive accuracy, or causality.

Methodologically, no additional delay compensation was applied beyond database time alignment, so modality and window-length differences remain potential sources of cohort bias. This choice keeps the extraction protocol simple and reproducible, but it may blur associations when pulse transit delays or non-invasive cuff timing differ from the optical waveform.

Future work should report signed correlations, subject-level and multiplicity-corrected inference, retained segment counts, sensitivity to filtering thresholds, out-of-domain prediction tests, and clinical covariates that may explain ICU-specific shifts. Such analyses are needed before consistent correlates can be considered reliable predictors in clinical deployment or used as evidence of physiological causation.

Table 1: Selected PPG features correlated with SBP and DBP. "Consistent" indicates minimum $|\rho| > 0.30$ and range ≤ 0.20.

Target	Feature	Mean $\lvert\rho\rvert$	Range $\lvert\rho\rvert$	Consistent
SBP	b/a	0.71	0.59–0.78	Yes
	d/a	0.65	0.59–0.71	Yes
	PDA-A_{13}	0.65	0.62–0.75	Yes
	AX	0.63	0.60–0.66	Yes
	AI_{gh}	0.56	0.51–0.62	Yes
	Y_{gh}	0.49	0.40–0.55	Yes
	S_{pf}	0.41	0.18–0.59	No
	PDA-T_{14}	0.41	0.20–0.60	No
	PDA-T_{15}	0.39	0.36–0.60	No
	Δn_{pf}	0.38	0.12–0.63	No
	PDA-T_{13}	0.37	0.32–0.56	No
DBP	Δn_{pf}	0.49	0.44–0.56	Yes
	PDA-W_1	0.49	0.44–0.56	Yes
	Δn_{up}	0.48	0.42–0.50	Yes
	N_e	0.46	0.40–0.47	Yes
	Δn_{gh}	0.46	0.40–0.52	Yes
	Δn_{ue}	0.44	0.40–0.50	Yes
	S_{pf}	0.46	0.12–0.59	No
	Δn_{pz}	0.44	0.29–0.64	No
	PDA-T_{14}	0.46	0.37–0.60	No
	PDA-T_{15}	0.44	0.37–0.60	No
	PDA-T_{13}	0.43	0.33–0.57	No

5. Conclusion

Across four heterogeneous datasets, signed SDPTG ratios, PDA-A_{13}, and selected wave-reflection features showed the most consistent SBP correlation magnitudes, whereas DBP associations were weaker and timing or slope features were more cohort-dependent.

A useful next step is to test whether models constrained to these consistent features lose less accuracy during external validation than models built from all available morphology descriptors.

Acknowledgments

This research has received partial financial support from public grants PID2021-123804OB-I00, PID2021-128525OB-I00 and PID2025-73302OB-I00 of the Spanish Government 10.13039/501100011033 jointly with the European Regional Development Fund (EU), SBPLY/24/180225/000184 from Junta de Comunidades de

Castilla-La Mancha and CIAICO/2023/200 from Generalitat Valenciana.

References

[1] Attivissimo F, D'Alessandro VI, De Palma L, Lanzolla AML, Di Nisio A. Non-Invasive Blood Pressure Sensing via Machine Learning. Sensors October 2023;23(19):8342. ISSN 1424-8220.

[2] Finnegan E, Davidson S, Harford M, Watkinson P, Tarassenko L, Villarroel M. Features from the photoplethysmogram and the electrocardiogram for estimating changes in blood pressure. Scientific Reports January 2023;13(1):986. ISSN 2045-2322.

[3] Elgendi M, Jost E, Alian A, Fletcher RR, Bomberg H, Eichenberger U, Menon C. Photoplethysmography Features Correlated with Blood Pressure Changes. Diagnostics October 2024;14(20):2309. ISSN 2075-4418.

[4] Chen Q, Yang X, Chen Y, Han X, Gong Z, Wang D, Zhang J. A blood pressure estimation approach based on single-channel photoplethysmography differential features. Biomedical Signal Processing and Control November 2024;97:106662. ISSN 1746-8094.

[5] Attivissimo F, De Palma L, Di Nisio A, Scarpetta M, Lanzolla AML. Photoplethysmography Signal Wavelet Enhancement and Novel Features Selection for Non-Invasive Cuff-Less Blood Pressure Monitoring. Sensors January 2023;23(4):2321. ISSN 1424-8220.

[6] Jiang S, Ashar P, Shandhi MMH, Dunn J. Demographic reporting in biosignal datasets: a comprehensive analysis of the PhysioNet open access database. The Lancet Digital Health November 2024; 6(11):e871–e878. ISSN 2589-7500.

[7] Mehta S, Kwatra N, Jain M, McDuff D. Examining the challenges of blood pressure estimation via photoplethysmogram. Scientific Reports August 2024; 14(1):18318. ISSN 2045-2322.

[8] Weber-Boisvert G, Gosselin B, Sandberg F. Intensive care photoplethysmogram datasets and machine-learning for blood pressure estimation: Generalization not guarantied. Frontiers in Physiology March 2023;14:1126957. ISSN 1664-042X.

[9] Mathew N, Shen Y, Hu R, Rahimi M, Zouridakis G. Benchmarking and Enhancing PPG-Based Cuffless Blood Pressure Estimation Methods, February 2026. ArXiv:2602.04725 [cs].

[10] Tóth B, Senti D, Ingolfsson TM, Zweidler J, Elsig A, Benini L, Li Y. Finetuning and Quantization of EEG-Based Foundational BioSignal Models on ECG and PPG Data for Blood Pressure Estimation, October 2025. ArXiv:2502.17460 [eess].

[11] Elgendi M, Haugg F, Fletcher RR, Allen J, Shin H, Alian A, Menon C. Recommendations for evaluating photoplethysmography-based algorithms for blood pressure assessment. Communications Medicine July 2024;4(1):140. ISSN 2730-664X.

[12] Liang Y, Chen Z, Liu G, Elgendi M. A new, short-recorded photoplethysmogram dataset for blood pressure monitoring in China. Scientific Data February 2018;5(1):180020. ISSN 2052-4463.

[13] Lee HC, Jung CW. VitalDB, a high-fidelity multi-parameter vital signs database in surgical patients. Type: dataset.

[14] Moulaeifard M, Charlton PH, Strodthoff N. MIMIC-III-Ext-PPG: A PPG Benchmark Dataset for Cardiorespiratory Analysis. Type: dataset.

[15] Moody B, Hao S, Gow B, Pollard T, Zong W, Mark R. MIMIC-IV Waveform Database. PhysioNet July 2022;Version 0.1.0.

[16] Sanches I, Gomes VV, Caetano C, Cabrera LSB, Cene VH, Beltrame T, Lee W, Baek S, Penatti OAB. MIMIC-BP: A curated dataset for blood pressure estimation. Scientific Data November 2024; 11(1):1233. ISSN 2052-4463.

[17] Marc-Derrien Y, Gren L, Dierschke K, Albin M, Gudmundsson A, Wierzbicka A, Sandberg F. Acute Cardiovascular Effects of Hydrotreated Vegetable Oil Exhaust. Frontiers in Physiology March 2022; 13:828311. ISSN 1664-042X.

[18] Ricci M, Fácila L, Alcaraz R, Rieta JJ, Sandberg F. Feature stability of PPG morphological descriptors across diverse clinical acquisition settings, 2026. Submitted to Computing in Cardiology.

Address for correspondence:

José J. Rieta

BioMIT.org, Electronic Engineering Department, Building 7F, Universitat Politècnica de València, 46022 Valencia, Spain.

e-mail: jjrieta@upv.es